

# Neutron Scattering Properties of Randomly Cross-Linked Polyisoprene Gels

Ferenc Horkay\*

*Section on Tissue Biophysics and Biomimetics, Laboratory of Integrative and Medical Biophysics, NICHD, National Institutes of Health, 13 South Drive, Bethesda, Maryland 20892*

Gregory B. McKenna

*Department of Chemical Engineering, Texas Tech University, Lubbock, Texas 79409*

Pascal Deschamps

*European Synchrotron Radiation Facility, B.P. 220, 38043 Grenoble, France*

Erik Geissler

*Laboratoire de Spectrométrie Physique CNRS UMR 5588, Université J. Fourier de Grenoble, B.P. 87, 38402 St. Martin d'Heres, France*

*Received February 17, 2000; Revised Manuscript Received April 17, 2000*

**ABSTRACT:** Measurements are reported of the osmotic swelling and elastic properties of cross-linked polyisoprene gels swollen in toluene, as a function of the polymer volume fraction  $\varphi$ . The swelling pressure and shear modulus results may be combined to yield the Flory–Huggins interaction parameter  $\chi$  for the cross-linked state of this system. It is found that  $\chi$  can be expressed as  $\chi = \chi_0 + \chi_1\varphi + \chi_2\varphi^2$ , where  $\chi_0 = 0.427$ ,  $\chi_1 = 0.000$ , and  $\chi_2 = 0.112$ . Small-angle neutron scattering (SANS) measurements are also reported for the same gels. The scattering intensity associated with the spontaneous thermodynamic concentration fluctuations in the gels is compared with that computed from the osmotic data. The agreement between the observed neutron intensities and the calculated values is good. The SANS measurements reveal two additional components to the scattered intensity: one due to the local elastic constraints of the cross-links and the other being caused by dense clusters that show no appreciable deformation when subjected to an external elastic strain field.

## Introduction

Considerable effort has been devoted to the understanding of the macroscopic properties of elastomers,<sup>1–4</sup> but rather fewer investigations have been reported into the local organization of the constituent polymer chains, the arrangements of which are at the root of the macroscopic properties. For such local investigations, techniques that give sub-microscopic spatial resolution are required, such as small-angle X-ray or neutron scattering. These techniques call for the introduction of a suitable contrast medium such as a solvent, to swell the network and separate the chain segments of one coil from those of another.

The aim of this paper is to shed light on the structure of polyisoprene networks in a lower resolution range than explored by wide-angle X-ray scattering (WAXS): such local order of the chains can be detected by small-angle neutron scattering (SANS). In the case of polymer solutions in which no long-range order is present, SANS detects concentration fluctuations of thermodynamic origin. These local thermal motions are the mechanism by which thermodynamic equilibrium is established, i.e., ensuring that the osmotic pressure is uniform throughout the sample. For systems displaying permanent concentration variations, such as cross-linked structures, the scattering response is enhanced over that of a solution. As the static structure has a direct bearing on the mechanical properties of these systems, its characterization is of great importance. To estimate the various contributions in the structure, it is necessary

to evaluate the scattering from the thermodynamic concentration fluctuations in the detected signal.<sup>5–7</sup> A knowledge of the mechanical properties and their relation to the local structure of the network is essential for the understanding and design of materials with specific properties.

Here, we investigate the concentration dependence of the osmotic swelling pressure and the elastic modulus of polyisoprene (PIP) networks swollen in toluene. We also measure the scattering signal over a wide range of concentrations for both polyisoprene solutions and gels. In addition, we examine the effect of anisotropic deformation on the scattering pattern of these gels.

## Theoretical Section

**Thermodynamics of Swollen Polymer Networks.** The present thermodynamic treatment of a cross-linked polymer is based on the hypothesis that the mixing and elastic components of the free energy are additive and separable,<sup>8,9</sup> i.e.

$$\Delta F_{\text{tot}} = \Delta F_{\text{mix}} + \Delta F_{\text{el}} \quad (1)$$

where  $\Delta F_{\text{tot}}$  is the total free energy. In the Flory–Huggins theory,<sup>9</sup> the mixing component in a polymer solution is given by

$$v_1^{-1} \partial \Delta F_{\text{mix}} / \partial n_1 = -\Pi_{\text{mix}} = (RT/v_1) [\ln(1 - \varphi) + (1 - F^{-1})\varphi + \chi\varphi^2] \quad (2)$$

where  $\Pi_{\text{mix}}$  is the osmotic mixing pressure exerted by

the  $n_1$  solvent molecules of molar volume  $v_1$ ,  $\varphi$  is the volume fraction of the polymer, and  $P$  is the degree of polymerization. For a cross-linked polymer  $P = \infty$ . The interaction parameter  $\chi$  is usually found to be concentration dependent and is accordingly expressed in the form of a truncated series

$$\chi = \chi_0 + \chi_1\varphi + \chi_2\varphi^2 \quad (3)$$

In the theory of Flory and Erman,<sup>10,11</sup> the elastic term in eq 1 adopts a complicated form which, in the phantom limit, simplifies to the expression proposed by James and Guth.<sup>12,13</sup> In this limit, where the chains can interpenetrate each other, the network component of the free energy is given by

$$\partial\Delta F_{el}/\partial n_1 = kT\zeta v_1\varphi^{1/3} \quad (4)$$

where  $\zeta$  is the cycle rank of the network. Several alternative expressions, based on different network models, have been proposed for the elastic term. For the purposes of this investigation, however, eq 4 gives an acceptable description of the elastic properties of the system.

In many real systems, aggregation of polymer chains and clustering of junction points is observed.<sup>14–16</sup> Such concentration nonuniformities are usually specific to the given system and depend on the conditions of preparation. None of the existing theories quantitatively describe the effect of the nonuniform distribution of the chains on the elastic and osmotic properties of the swollen network.

**Scattering from Polymer Solutions and Gels.** In a neutral polymer solution, the normalized intensity of elastically scattered radiation at small transfer wave vectors is inversely proportional to the osmotic compressibility,  $K_{os} = \varphi(\partial\Pi/\partial\varphi)$ ; thus

$$I(Q) = (\Delta\rho^2 kT\varphi^2/K_{os})(1 + Q^2\xi^2)^{-1} \quad (5)$$

where  $Q [= (4\pi/\lambda) \sin(\theta/2)]$ ,  $\lambda$  being the incident neutron wavelength and  $\theta$  the scattering angle] is the scattering wave vector,  $\Pi$  is the osmotic pressure,  $\xi$  is the correlation length characterizing the distance between the structural elements in the system, and  $\rho^2 = (\rho_p - \rho_s)^2$  is a contrast factor. In SANS experiments  $(\rho_p - \rho_s)$  is the difference in the coherent scattering length densities between the polymer and solvent. From the known densities of PIP and deuterated toluene and the tabulated scattering lengths of their constituent nuclei,<sup>17</sup> the contrast factor is found to be

$$\Delta\rho^2 = (\rho_p - \rho_s)^2 = 2.92 \times 10^{21} \text{ cm}^{-4} \quad (6)$$

From eq 1 it follows that, in a gel, the pressure exerted by the network on its surroundings as it absorbs solvent molecules is not simply the osmotic pressure  $\Pi_{mix}$  but rather the swelling pressure,

$$\omega = \Pi_{mix} - G \quad (7)$$

where  $G$  is the elastic modulus of the swollen network. The scattering of radiation by osmotic fluctuations is then governed by the longitudinal osmotic modulus

$$M_{os} = \varphi \partial\omega/\partial\varphi + \frac{4}{3}G \quad (8)$$

In gels the total scattered intensity is usually higher

than in the corresponding (un-cross-linked) polymer solutions. The excess intensity arises from an inhomogeneous distribution of the network structure.<sup>18,19</sup> In gels with light to moderate cross-linking, such static nonuniformities are not expected to contribute significantly to the osmotic properties of the swollen network: the thermodynamics of gels are primarily governed by the freely fluctuating (solution-like) part of the system.<sup>5–7,18,20,21</sup>

## Experimental Details

**Gel Preparation.** The poly(isoprene) gels were made according to a method used by McKenna et al.<sup>2</sup> A poly(*cis*-isoprene) (Polysciences Inc., catalog no. 4569, lot no. 402530) sample was mixed in toluene solution with differing amounts of cross-link agent (dicumyl peroxide): 0.5, 2, 5, and 10 parts per hundred. The specimens were dried and then baked in an oven at 150 °C for 2 h.

For the calculation of the polymer volume fractions  $\varphi$  in the neutron scattering measurements, the densities of the pure components were taken to be  $d_{PIP} = 0.895 \text{ g cm}^{-3}$  and  $d_{\text{tolueneD}} = 0.9423 \text{ g cm}^{-3}$ .

**Small-Angle Neutron Scattering Measurements.** The SANS measurements were performed on the NG3 instrument at NIST, Gaithersburg, using an incident wavelength of 6 Å and selector bandwidth of 10%. The detector was placed at three distances, 1.8, 6, and 13 m from the sample. The  $Q$  range explored was  $0.005 \text{ \AA}^{-1} < Q < 0.23 \text{ \AA}^{-1}$ , with counting times of between 10 min and 1 h. The ambient temperature during the experiments was  $25 \pm 1 \text{ }^\circ\text{C}$ .

Deuterated toluene was used as solvent. The sample cell consisted of 1 mm thick quartz windows separated by a 1 mm thick spacer, sealed by a Viton O-ring. After radial averaging, corrections for incoherent background, detector response, and cell window scattering were applied.<sup>6</sup> Calibration of the scattered neutron intensity was performed using the signal from standard samples of silica aerogel.<sup>22</sup>

Anisotropic samples were made by cutting an ellipse out of a sheet of the dry elastomer and allowing it to swell in excess solvent inside the circular sample holder. As the gel expands in the confined space, swelling remains isotropic until the major axis of the ellipse touches the inner diameter of the cell (17.5 mm). Thereafter the expansion is anisotropic. In the direction perpendicular to the neutron beam, the final stretch ratio  $\Lambda$  is thus equal to the axial ratio of the ellipse when it first comes into contact with the sample holder. The resulting circular sample is then homogeneously strained. As small-angle scattering experiments are insensitive to strain in the direction parallel to the neutron beam, the only effect of the confinement in this direction is to limit the final concentration of the sample.

**X-rays.** Wide-angle X-ray scattering confirms the absence of crystallization in this material. These measurements were performed using D43 beam-line at the DCI synchrotron radiation source at LURE, Orsay, France. The bandwidth of the monochromator was  $\Delta\lambda/\lambda = 3 \times 10^{-4}$ , working at a wavelength  $\lambda = 0.1 \text{ nm}$ , and an image plate was used as a detector. Figure 1 shows the region of the X-ray spectrum around the amorphous halo, which spans the (200), (120), and (201) Bragg reflections from this system.<sup>23,24</sup> No crystalline peak is detectable.

**Osmotic and Mechanical Measurements.** The swelling pressure of the gels was measured as a function of the polymer concentration using a modified deswelling method.<sup>25</sup> Gels were equilibrated with polymer solutions of known osmotic pressure in toluene.<sup>26</sup> A semipermeable membrane was inserted between the gel and the solution to prevent diffusion of the polymer molecules into the swollen network. In the present case poly(vinyl acetate) ( $M_w = 140\,000$ ) was used to adjust the solvent activity. At equilibrium, the swelling pressure  $\omega$  of the gels is equal to the osmotic pressure of the external solution,

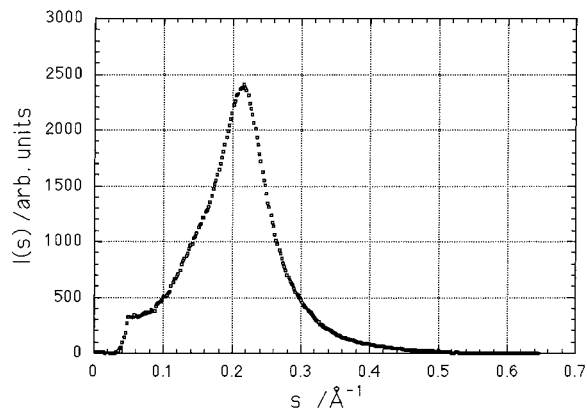


**Figure 1.** WAXS spectrum of the dry PIP sample obtained with an image plate at the D43 beam-line at LURE, Orsay ( $s = (2/\lambda) \sin(\theta/2)$ , the wavelength of the incident radiation being  $\lambda = 0.9 \text{ \AA}$ ).

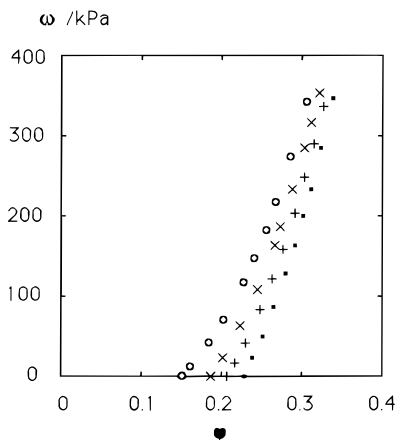


**Figure 2.** Swelling pressure of four PIP networks with different cross-link densities, swollen to various degrees in toluene at 25 °C.

the values of which are known:<sup>26</sup>

$$\omega = \Pi_{\text{ext}} \tag{9}$$

The shear modulus measurements were performed on isometric cylindrical gel specimens prepared in a special mold. Swollen networks were uniaxially compressed (at constant volume) between two parallel flat plates. The stress-strain data were determined in the range of deformation ratio  $0.7 < \Lambda < 1$ . The absence of volume change and barrel distortion was checked. The results were analyzed using the relation

$$\sigma = C_1(\Lambda - \Lambda^{-2}) \tag{10}$$

where  $\sigma$  is the nominal stress (related to the undeformed cross section of the gel cylinder) and the constant  $C_1$  is equal to the shear modulus of the swollen network.

**Results and Discussion**

**Osmotic and Mechanical Measurements.** In Figure 2 the measured values of the swelling pressure  $\omega$  are plotted as a function of polymer volume fraction  $\phi$ , for four PIP networks prepared with different amounts of cross-link agent. Figure 3 shows the shear moduli of these gels, measured at the same degrees of swelling as in Figure 2, and plotted in a double-logarithmic representation. To a good approximation the data points form a set of straight lines with a slope of  $1/3$ , in accordance with the phantom network approximation of expression 4.<sup>8,12,13</sup> Linear regression through the

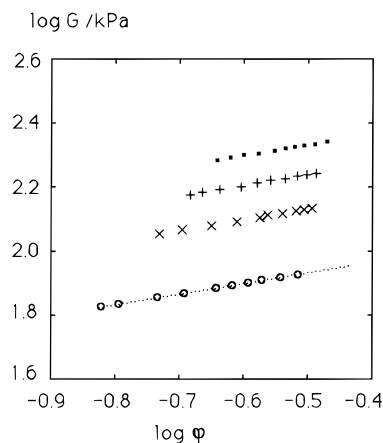


**Figure 3.** Shear modulus  $G$  as a function of polymer volume fraction for polyisoprene gels swollen in toluene. The slope of the line of linear regression through the lowest data set is  $0.332 \pm 0.002$ .

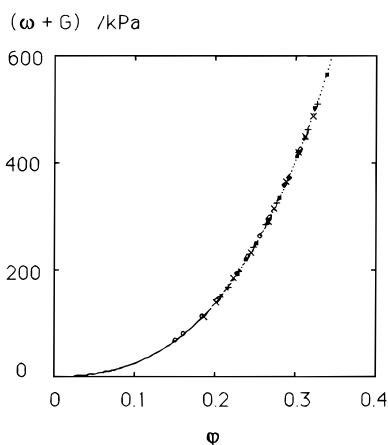


**Figure 4.** Fit of osmotic component of swelling pressure  $\Pi = \omega + G$  to expression 2 for the swelling pressure data for the four networks in Figures 2 and 3.

points for the most lightly cross-linked network (circles) yields

$$G = G_0 \phi^m \tag{11}$$

where  $G_0 = 125.2 \pm 0.3 \text{ kPa}$  and  $m = 0.332 \pm 0.002$ . This sample was used for the neutron scattering experiment described below.

In the swollen network, the mixing contribution to the swelling pressure is found from the relation

$$\Pi_{\text{mix}} = \omega + G \tag{12}$$

where both  $\omega$  and  $G$  are found by direct measurement. Figure 4 shows  $(\omega + G)$  as a function of  $\phi$  for the same four sets of gels as in Figures 2 and 3. The points lie on a master curve. The continuous curve through the points is the least-squares fit to the data of the Flory–Huggins expression (2), which yields the following values for the interaction parameters

$$\chi_0 = 0.427, \quad \chi_1 = 0.000, \quad \chi_2 = 0.112 \tag{13}$$

The existence of the master curve for the concentration dependence of the quantity  $(\omega + G)$  shows that it is insensitive to variations in cross-link density. This shows that the dominant factor is the polymer concentration. The above  $\chi$  values exceed those obtained for

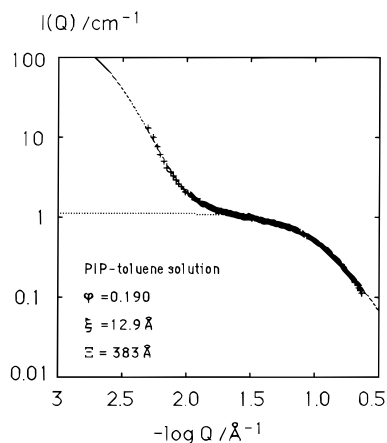


**Figure 5.** SANS spectrum of an un-cross-linked PIP-toluene solution at  $\varphi = 0.190$ . The strong extra scattering at low  $Q$  results from the presence of local inhomogeneities (amorphous clusters) in the solution.

the corresponding solutions of un-cross-linked poly(isoprene), in accordance with previous results of McKenna et al.<sup>2,3</sup> and other groups.<sup>5,6</sup>

**SANS Measurements on Isotropic Gels.** Small-angle neutron scattering was used to investigate the small-scale structures.<sup>22</sup> For other gel systems,<sup>5-7</sup> we have previously found that the scattering spectrum can be satisfactorily described using the expression

$$I(Q) = \Delta\rho^2 \{ (kT\varphi^2/M_{os})(1 + Q^2\xi^2)^{-1} + B(1 + Q^2\xi^2)^{-2} \} \quad (14)$$

As indicated above, the first term describes the scattering from thermally induced motions of the chains in the solvent. The second term represents longer range static variations in concentration due to the permanent elastic constraints inside the network. The latter term is a Debye–Bueche expression,<sup>27</sup> in which the long correlation length  $\Xi$  describes the spatial range of the elastic deformations.

In the present PIP–toluene systems, both the gels and the un-cross-linked solutions display slight haze, indicating the presence of clusters whose size is comparable with the wavelength of visible light. Cluster formation has already been observed in various polymer solutions by several authors,<sup>28-31</sup> which was attributed to specific interactions between polymer segments and the solvent molecules. The presence of clusters is confirmed here also by the SANS spectrum shown in Figure 5, where in addition to the expected thermodynamic term (dotted line) strong extra scattering is visible at low  $Q$ . Use of eq 15 to model the total response yields a satisfactory fit to the data (continuous line). The SANS spectrum of the dry network, however, also displays an excess scattering feature at small  $Q$ , similar to that in the solutions. This result indicates that in the present case solvent-induced specific interactions are not significant.

The influence of these clusters on the SANS spectrum persists into the cross-linked gels. Application of eq 14 to the PIP gel spectra, however, produces unacceptably poor fits, which indicates that two correlation lengths are inadequate to describe the system. As discussed earlier, in addition to the features observed in the solution, gel spectra in general contain a structural element due to frozen-in elastic constraints:<sup>18</sup> the latter can be described by concentration fluctuations of mean-

square amplitude  $\langle\delta\varphi^2\rangle$  with a spatial range  $\Xi_1$ . Neutron scattering in these PIP gels thus reveals a hierarchy of characteristic lengths: the thermal correlation length  $\xi$ , the elastic correlation length  $\Xi_1$ , and the new length  $\Xi_2$  that characterizes the clusters, similar to those observed in the solution. Since it is found that static contributions can be described by the Debye–Bueche formalism,<sup>27</sup> in the case of the present PIP–toluene system, it is natural to extend eq 14 by writing

$$I(Q) = \Delta\rho^2 \{ A(1 + Q^2\xi^2)^{-1} + B_1(1 + Q^2\xi_1^2)^{-2} + B_2(1 + Q^2\xi_2^2)^{-2} \} \quad (15)$$

in which the amplitude of the thermodynamic term is now<sup>7</sup>  $A = kT\varphi^2/M_{os}$ , while  $B_1 = 8\pi\langle\delta\varphi^2\rangle\xi_1^3$ .  $B_2$  is the intensity scattered by the clusters. As the WAXS measurements reveal no crystallinity, these clusters must be amorphous.

From eqs 2, 7, 8, 11, and 13, the longitudinal elastic modulus,  $M_{os}$ , can be expressed independently in terms of the measurements of the swelling pressure and the elastic modulus

$$M_{os} = \varphi^2(RTv_1) \{ 1/(1 - \varphi) - 2\chi_0 - 3\chi_1\varphi - 4\chi_2\varphi^2 \} + G_0\varphi^{1/3} \quad (16)$$

We are now in a position to compare the osmotic component in the SANS spectra (i.e., the first term in eq 15) with the results derived from macroscopic observations. Substitution of the parameters  $\chi_1$  and  $G_0$  from eqs 11 and 13 into expression 16, together with the calculated value of the contrast factor (eq 6), yields the theoretical intensity scattered by the thermodynamic concentration fluctuations in the swollen network.

In Figure 6a–c the SANS spectra of the PIP gels are shown for different degrees of swelling in deuterated toluene, together with the corresponding fits of eq 15. The parameters are listed in Table 1. In each figure, the thermodynamic component (of amplitude  $A$ ) of this fit is shown as a dotted line. In these figures the arrows placed against the ordinate axis indicate the value of the intensity of the thermal contribution calculated from the osmotic and mechanical measurements with eq 16. For the more swollen gels, the agreement between the values of the parameter  $A$  in Figure 6 and those evaluated from the macroscopic measurements is satisfactory. Although the volume fraction of the most concentrated gel,  $\varphi = 0.491$ , lies outside the range of the osmotic swelling pressure measurements ( $0.15 < \varphi < 0.35$ ), the thermodynamic component was estimated using the same parameters as in Figure 6a,b (arrow). In this extrapolated region, the value of the intensity thus calculated is larger by a factor of 2 than that observed. This discrepancy may be attributed to other terms that become significant in the highly concentrated region. We conclude that in the concentration range for which the osmotic measurements apply the agreement between swelling pressure and SANS measurements is reasonable.

The large-scale structures in these gels thus consist of two contributions: the first is caused by the competition of the osmotic pressure and the residual elastic constraints frozen into the network, while the second appears to be associated with the presence of dense clusters in this particular system. In the most swollen



**Table 1. Parameters from Fits of Eq 15 to SANS Spectra**

sample	vol fract $\varphi$	$\Delta\rho^2 A/\text{cm}^{-1}$	$\Delta\rho^2 B_1/\text{cm}^{-1}$	$\Delta\rho^2 B_2/\text{cm}^{-1}$	$\xi/\text{\AA}$	$\Xi_1/\text{\AA}$	$\Xi_2/\text{\AA}$	$\langle\delta\varphi^2\rangle/\varphi$
gel 1	0.166	1.2	2.0	290	11.2	52	380	0.083
gel 2	0.224	1.0	1.8	260	8.8	43	370	0.079
gel 3	0.491	0.21	0.45	142	6.2	47	480	0.016
solution 1	0.192	1.10		233	12.9		383	
solution 2	0.273	0.75		32	8.4		196	

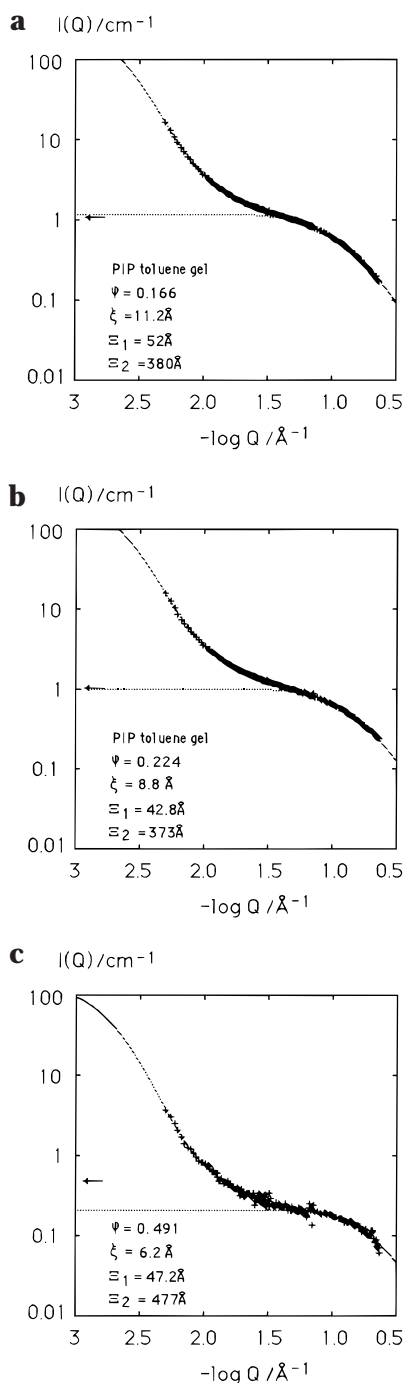


**Figure 6.** (a) SANS spectrum from a fully swollen PIP–toluene gel at  $\varphi = 0.166$ . The continuous curves are the fits of eq 15 through the data, and the dotted line is the thermodynamic component in this fit. The horizontal arrow at the coordinate axis indicates the scattering intensity calculated from the macroscopic osmotic and mechanical measurements. (b) SANS spectrum from a swollen PIP–toluene gel at  $\varphi = 0.224$ , and the corresponding fit to eq 15. (c) SANS spectrum from a swollen PIP–toluene gel at  $\varphi = 0.491$  and the corresponding fit to eq 15.

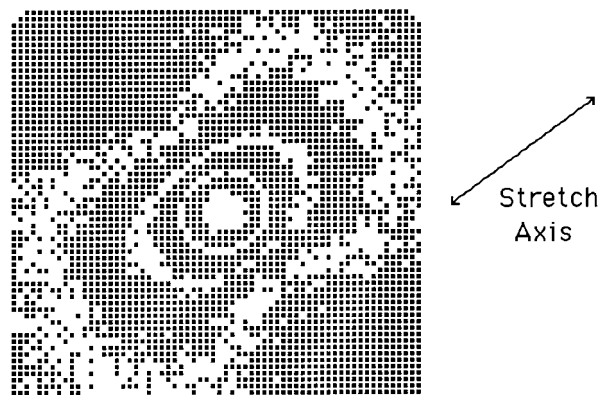


**Figure 7.** Isointensity scattering pattern from a PIP gel swollen in toluene, stretched along the diagonal direction indicated in the figure by a ratio  $\Lambda = 2$ , as described in the Experimental Section. Sample detector distance  $d = 13$  m, incident wavelength  $6\text{ \AA}$ . The levels of the contours are 800, 1500, and 5000 counts.

sample, the value found for the relative amplitude of the frozen fluctuations,  $\langle\delta\varphi^2\rangle/\varphi^2$ , is approximately 10%.

**Scattering from Uniaxially Stretched Gels.** In the previous paragraph we introduced two static correlation lengths: the first describes the elastic constraints imposed by the cross-links, while the second accounts for large amorphous clusters. If this picture is correct, the variation of these characteristic lengths under anisotropic deformation will be different. Under uniaxial deformation the thermodynamic correlation length,  $\xi$ , is expected to be unaffected since the osmotic pressure is isotropic. The static correlation length  $\Xi_1$ , however, should display anisotropy, since it transmits the elastic strain field in the network. As to the second static correlation length  $\Xi_2$ , any deformation of the amorphous clusters will produce anisotropy in the corresponding region of the scattering pattern. To explore the different behavior of these length scales, we performed SANS measurements on a uniaxially stretched sample. This observation provides a straightforward method of distinguishing differences in elastic response of these two superstructures in the perpendicular and parallel directions to the stretch axis.

Figure 7 shows the scattering pattern of a uniaxially stretched PIP gel, with a stretching ratio of roughly 2 along the diagonal axis indicated in the diagram. The isointensity lines of the central region of the detector form a figure-eight or “butterfly” pattern<sup>32–35</sup> in the region  $Q\xi < 1$ . In the outer range of this figure the thermodynamic component of the scattering, which is isotropic, is masked by that from the elastic deformations, i.e., the intermediate correlation length  $\Xi_1$ . At the center of the pattern, however, the anisotropic elastic contribution is in turn overwhelmed by the strong excess intensity arising from the clusters. The latter is isotropic. This finding corroborates our assumption that the two length scales  $\Xi_1$  and  $\Xi_2$  required to describe the static response of this system indeed correspond to different phenomena. The novel feature of Figure 7 is

that the innermost region of the butterfly pattern is isotropic in the lowest  $Q$  range. Thus,  $\Xi_1$  deforms in response to the overall deformation of the gel, while  $\Xi_2$ , describing rigid amorphous clusters, is practically unaffected by the overall strain field prevailing in the sample.

### Conclusions

Osmotic swelling pressure and elastic modulus measurements were made on a series of poly(isoprene) gels swollen in toluene. The cross-link density was varied in a wide range from 0.5% to 10% dicumyl peroxide. It was found that the concentration dependence of the mixing pressure (i.e., the sum of the swelling pressure  $\omega$  and the elastic modulus  $G$ ) forms a master curve that is insensitive to the cross-link density over the range of observation. The numerical values of the Flory–Huggins interaction parameters of the gels determined from these data are larger than those for poly(isoprene) toluene solutions reported in the literature. This finding is in accordance with previous results of McKenna et al.<sup>2,3</sup> and other groups.<sup>5,6</sup>

Neutron scattering measurements were also performed on the same gel system at different degrees of swelling. The gel signal can be described by three length scales corresponding to different structural elements. These are the thermodynamic correlation length  $\xi$  related to the osmotic component of the swelling pressure, the correlation length  $\Xi_1$  connected with residual elastic constraints generated by the cross-links, and a length  $\Xi_2$  of the order of several tens of nanometers describing an extended rigid structure. The absence of crystallinity in these samples leads us to conclude that the large-scale structures are amorphous. Using this approach, we find that the intensity of the thermodynamic component is in good agreement with that calculated from the swelling pressure and elastic modulus measurements.

Differences in the elastic response of the two static structural components are revealed by small-angle neutron scattering from anisotropically deformed samples: the elastic structures give rise to a butterfly pattern; at low  $Q$ , the latter is masked by the isotropic scattering from the undeformed clusters.

**Acknowledgment.** We acknowledge the support of the National Institute of Standards and Technology, U.S. Department of Commerce, in providing the neutron research facilities used in this experiment. This work is based upon activities supported by the National Science Foundation under Agreement DMR-9423101. We are grateful to B. Hammouda for his invaluable help. We also thank LURE, Orsay, for access to the D43 beam line.

### References and Notes

- (1) McKenna, G. B.; Crissman, J. M. *J. Polym. Sci., Polym. Phys. Ed.* **1997**, *35*, 817.
- (2) McKenna, G. B.; Flynn, K. M.; Chen, Y. H. *Macromolecules* **1989**, *22*, 4507.
- (3) McKenna, G. B.; Flynn, K. M.; Chen, Y. H. *Polymer* **1993**, *31*, 1937.
- (4) Douglas, F. F.; McKenna, G. B. In *Elastomeric Polymer Networks*; Mark, J. E., Erman, B., Eds.; Prentice Hall: Englewood Cliffs, NJ, 1992; p 327.
- (5) Mallam, S.; Horkay, F.; Hecht, A. M.; Rennie, A. R.; Geissler, E. *Macromolecules* **1991**, *23*, 543.
- (6) Horkay, F.; Hecht, A. M.; Mallam, S.; Geissler, E.; Rennie, A. R. *Macromolecules* **1991**, *24*, 2896.
- (7) Geissler, E.; Horkay, F.; Hecht, A. M.; Rochas, C.; Lindner, P.; Bourgaux, C.; Couarraze, G. *Polymer* **1997**, *38*, 15.
- (8) Flory, P. J. *J. Chem. Phys.* **1977**, *60*, 5720.
- (9) Flory, P. J. *Principles of Polymer Chemistry*; Cornell: Ithaca, NY, 1953.
- (10) Flory, P. J.; Erman, B. *Macromolecules* **1984**, *15*, 800.
- (11) Erman, B.; Flory, P. J. *Macromolecules* **1984**, *15*, 806.
- (12) James, H. M.; Guth, E. J. *J. Chem. Phys.* **1943**, *11*, 455.
- (13) Treloar, L. R. G. *The Physics of Rubber Elasticity*, 3rd ed.; Clarendon: Oxford, 1975.
- (14) Dušek, K.; Prins, W. *Adv. Polym. Sci.* **1969**, *6*, 1.
- (15) Geissler, E.; Hecht, A. M.; Duplessix, R. *J. Polym. Sci., Polym. Phys. Ed.* **1982**, *20*, 226.
- (16) Hecht, A. M.; Duplessix, R.; Geissler, E. *Macromolecules* **1985**, *18*, 2167.
- (17) Sears, V. F. *Neutron News* **1992**, *3* (3), 26.
- (18) Geissler, E.; Horkay, F.; Hecht, A. M. *Phys. Rev. Lett.* **1993**, *71*, 645.
- (19) Bastide, J.; Candau, S. J. In *Physical Properties of Polymeric Gels*; Cohen Addad, J. P., Ed.; Wiley: Chichester, 1996; p 143.
- (20) Geissler, E.; Horkay, F.; Hecht, A. M. *Macromolecules* **1991**, *24*, 6006.
- (21) NIST Cold Neutron Research Facility. NG3 and NG7 30-meter SANS Instruments Data Acquisition Manual, Jan 1996.
- (22) Tomlin, D. W.; Roland, C. M. *Polymer* **1993**, *34*, 2665.
- (23) Balta-Calleja, F. J.; Vonk, C. G. In *X-ray Scattering of Synthetic Polymers*; Jenkins, A. D., Ed.; Polymer Science Library 8; Elsevier: Amsterdam, 1989.
- (24) Nagy, M.; Horkay, F. *Acta Chim. Acad. Sci. Hung.* **1980**, *104*, 49.
- (25) Horkay, F.; Zrinyi, M. *Macromolecules* **1982**, *15*, 1306.
- (26) Vink, H. *Eur. Polym. J.* **1971**, *7*, 1411.
- (27) Debye, P.; Bueche, R. M. *J. Appl. Phys.* **1949**, *20*, 518.
- (28) François, J.; Gan, Y. S.; Guenet, J. M. *Macromolecules* **1986**, *19*, 173.
- (29) Gan, Y. S.; François, J.; Guenet, J. M. *Macromolecules* **1986**, *19*, 2755.
- (30) Guenet, J. M.; Kein, M.; Menelle, A. *Macromolecules* **1989**, *22*, 494.
- (31) Izumi, Y.; Katano, S.; Funahashi, S.; Furusaka, M.; Arai, M. *Physica B* **1992**, *181*, 539.
- (32) Oeser, R. *Polymer Motion in Dense Systems, Springer Proc. Phys.* **1988**, *29*, 104.
- (33) Rouf, C.; Bastide, J.; Pujol, J. M.; Schosseler, F.; Munch, J. P. *Phys. Rev. Lett.* **1994**, *73*, 830.
- (34) Geissler, E.; Horkay, F.; Hecht, A. M. *J. Chem. Phys.* **1995**, *102*, 9127.
- (35) Ramzi, A.; Zielinski, F.; Bastide, J.; Boué, F. *Macromolecules* **1995**, *28*, 3570.